RESEARCH ARTICLE

Viral Pathogen-Associated Molecular Patterns Regulate Blood-Brain Barrier Integrity via Competing Innate Cytokine Signals

Brian P. Daniels,[a] David W. Holman,[b] Lillian Cruz-Orengo,[b] Harsha Jujjavarapu,[b] Douglas M. Durrant,[b] Robyn S. Klein[a,b,c]

Department of Anatomy and Neurobiology,[a] Department of Internal Medicine,[b] and Department of Pathology and Immunology,[c] Washington University School of Medicine, St. Louis, Missouri, USA

ABSTRACT **Pattern recognition receptor (PRR) detection of pathogen-associated molecular patterns (PAMPs), such as viral RNA, drives innate immune responses against West Nile virus (WNV), an emerging neurotropic pathogen. Here we demonstrate that WNV PAMPs orchestrate endothelial responses to WNV via competing innate immune cytokine signals at the blood-brain barrier (BBB), a multicellular interface with highly specialized brain endothelial cells that normally prevents pathogen entry. While Th1 cytokines increase the permeability of endothelial barriers, type I interferon (IFN) promoted and stabilized BBB function. Induction of innate cytokines by pattern recognition pathways directly regulated BBB permeability and tight junction formation via balanced activation of the small GTPases Rac1 and RhoA, which in turn regulated the transendothelial trafficking of WNV. *In vivo*, mice with attenuated type I IFN signaling or IFN induction (*Ifnar*$^{-/-}$ *Irf7*$^{-/-}$) exhibited enhanced BBB permeability and tight junction dysregulation after WNV infection. Together, these data provide new insight into host-pathogen interactions at the BBB during neurotropic viral infection.**

IMPORTANCE **West Nile virus (WNV) is an emerging pathogen capable of infecting the central nervous system (CNS), causing fatal encephalitis. However, the mechanisms that control the ability of WNV to cross the blood-brain barrier (BBB) and access the CNS are unclear. In this study, we show that detection of WNV by host tissues induces innate immune cytokine expression at the BBB, regulating BBB structure and function and impacting transendothelial trafficking of WNV. This regulatory effect is shown to happen rapidly following exposure to virus, to occur independently of viral replication within BBB cells, and to require the signaling of cytoskeletal regulatory Rho GTPases. These results provide new understanding of host-pathogen interactions at the BBB during viral encephalitis.**

Received 12 June 2014 **Accepted** 29 July 2014 **Published** 26 August 2014

Citation Daniels BP, Holman DW, Cruz-Orengo L, Jujjavarapu H, Durrant DM, Klein RS. 2014. Viral pathogen-associated molecular patterns regulate blood-brain barrier integrity via competing innate cytokine signals. mBio 5(5):e01476-14. doi:10.1128/mBio.01476-14.

Editor Diane Griffin, Johns Hopkins University School of Public Health

Address correspondence to Robyn S. Klein, rklein@dom.wustl.edu.

The central nervous system (CNS) is normally protected from pathogens by the blood-brain barrier (BBB), which is composed of brain microvascular endothelial cells (BMECs) joined by tight junctions (TJs). TJs are formed by the intercellular association of transmembrane proteins, including claudins and occludins, whose anchoring to the endothelial cytoskeletal network by adaptor proteins, including the zonula occludens family, represents a major regulatory mechanism by which paracellular permeability is controlled (1). Viruses may cross the BBB via several routes, including direct infection of BMECs, trans- or paracellular viral trafficking across the endothelium (2), or entry of infected peripheral leukocytes (3, 4). Trafficking of virus across the BBB is likely made possible by enhanced permeability of the BBB endothelium, caused either directly by viral factors or indirectly by host immune factors, including innate cytokines such as tumor necrosis factor alpha (TNF-α) and interleukin-1β (IL-1β) (5, 6). However, the mechanistic explanation of this effect and the functions of innate immune responses at the BBB interface during viral infections have not been explored.

West Nile virus (WNV), a mosquito-borne flavivirus, is the most common cause of epidemic viral encephalitis in the United States (7). Following infection, the pattern recognition receptors (PRRs) TLR3, TLR7, RIG-I, and MDA5 are key sensors of WNV pathogen-associated molecular patterns (PAMPs), inducing the expression of innate Th1 cytokines that limit viral replication, facilitate antigen presentation, and direct the trafficking of antiviral leukocytes (8, 9). Studies with mice have shown that TNF-α signaling is key for CD8$^+$ T cell-mediated clearance of WNV from the CNS (10), as well as protection from CXCR3-mediated apoptosis in neurons (11). Likewise, IL-1β signaling has been shown to limit WNV replication in neurons (12) and is essential for dendritic-cell-mediated reactivation of WNV-specific T cells in the CNS (13). Despite these beneficial effects in the CNS, Th1 cytokine signaling can also contribute to neuropathology, including disruption of the BBB (6, 14).

PRR activation also induces the expression of type I interferons (IFN-α and IFN-β) that share a type I IFN receptor (IFNAR). PRR-mediated expression of IFN ligands results in the amplification of type I IFN signals via both autocrine and paracrine signaling through IFNAR, which stimulates further IFN ligand expression and an array of IFN-stimulated antiviral and immunomodulatory genes (15). Type I IFNs act directly as potent suppres-

sors of viral replication (16) and indirectly by promoting host adaptive immune responses (17). Thus, mice lacking type I IFN receptors, ligands, and key transcription factors exhibit expanded viral tropism and replication, resulting in accelerated and enhanced death (16, 18, 19). In the context of CNS autoimmunity, type I IFNs can enhance BBB function and are used clinically in humans to prevent the CNS entry of autoreactive leukocytes in patients with multiple sclerosis (20, 21). However, the functions of type I IFN at the BBB interface during viral infections of the CNS have not yet been explored.

Here, we demonstrate a novel mechanism underlying the dynamic regulation of BBB structure and function by innate cytokines during viral encephalitis. Using an *in vitro* BBB model, we show that, in the presence of WNV, the induction of type I IFN directly regulates endothelial permeability and TJ formation via regulation of the small GTPases Rac1 and RhoA and indirectly via suppression of barrier-dysregulating effects of TNF-α and IL-1β. This regulatory regimen modulates transendothelial WNV trafficking, as type I IFN responses significantly decreased the movement of virus across an intact barrier *in vitro*, while TNF-α and IL-1β increased this crossing. *In vivo*, genetic attenuation of type I IFN signaling resulted in enhanced BBB permeability with associated TJ disruption following peripheral or intracranial (i.c.) inoculation with WNV. Together, these data demonstrate an additional, previously undescribed, regulatory role for PRR-mediated cytokine expression at the BBB during WNV infection.

RESULTS

Innate cytokines differentially regulate barrier function following WNV infection. To assess the kinetics of BBB permeability following murine WNV infection, we utilized an established model of WNV neuroinvasive disease in which 5-week-old C57BL/6 mice are subcutaneously infected in the footpad with 10^2 PFU of a virulent strain of WNV-NY. Five-week-old mice uniformly develop CNS infection, with detectable CNS viral loads first emerging ~6 days following infection (22, 23) (see Fig. S1A in the supplemental material). Fluorometric assessment of BBB permeability following the intraperitoneal (i.p.) administration of sodium fluorescein revealed that BBB permeability increased significantly over the course of peripheral infection (days 0 to 4) in all of the CNS regions analyzed (Fig. 1A). Of interest, BBB permeability exhibited a significant decrease at day 6 in cortical and subcortical cerebral tissues, coincident with the timing of detection of virus within the CNS (see Fig. S1A). After this, BBB permeability rebounded and returned to elevated levels on day 8, coinciding with increased trafficking of leukocytes into the CNS (22).

The biphasic kinetics of BBB permeability after WNV infection suggested potentially differential regulation of the BBB by viral and host factors over the course of infection. To assess this, we utilized a standard Transwell *in vitro* BBB system in which primary murine BMECs are grown on a porous filter membrane in a chamber suspended above primary murine astrocytes. The integrity of the endothelial barrier is assessed via electrode recording of transendothelial electrical resistance (TEER). We treated *in vitro* BBB cultures in the top (BMEC-only) chamber overnight with cytokines or infected them for 6 h at a multiplicity of infection (MOI) of 0.01 with WNV that had been purified via ultracentrifugation through a sucrose gradient. We utilized a low MOI for BMEC experiments in light of the relatively low viremia present in mammalian hosts during WNV infection (24) and the fact that high MOIs can trigger fast necrotic cell death (25), compromising monolayer integrity and confounding the interpretation of TEER results. Similarly, 6-h infections were chosen because this period of time is insufficient for completion of the viral life cycle and induction of apoptosis in BMECs, as assessed via multistep growth curves and terminal deoxynucleotidyltransferase-mediated dUTP-biotin nick end labeling (TUNEL) staining (see Fig. S1B and C in the supplemental material). Treatment with Th1 cytokines TNF-α (100 ng/ml), IL-1β (100 ng/ml), and IFN-γ (100 ng/ml) decreased TEER, while IFN-β (100 pg/ml) and WNV infection both significantly enhanced TEER (Fig. 1B). TEER effects induced by Th1 cytokines could be rescued by subsequent infection with WNV, while infection of IFN-β-treated cultures produced no additional increase in TEER (Fig. 1B). Similar to WNV, addition of IFN-β to cultures pretreated with Th1 cytokines also rescued TEER (Fig. 1C). These data suggest that WNV infection may increase TEER either via type I IFN or through convergent mechanisms.

To assess whether type I IFN expression by BMECs and/or astrocytes contributes to increasing TEER, we performed checkerboard experiments with BMECs and astrocytes isolated from wild-type (WT) and/or *Ifnar*$^{-/-}$ mice. While TEER increased after 6 h of infection in cultures with WT BMECs, similarly infected cultures generated with *Ifnar*$^{-/-}$ BMECs instead exhibited significant reductions in TEER (Fig. 1D). While type I IFN signaling in BMECs robustly controlled TEER responses after infection, type I IFN signaling in astrocytes produced smaller but significant modulations of TEER responses as well. Experiments with neutralizing antibodies to IFNAR and IFN ligands recapitulated the results obtained with *Ifnar*$^{-/-}$ BMECs (data not shown). Given the dramatic change in TEER responses in the absence of type I IFN signaling, we next assessed the expression of innate cytokines in BMECs following infection. In WT BBB cultures, the expression of both IFN-β and TNF-α is induced within 6 h in the top chambers of BBB cultures, with mostly undetectable levels of IL-1β. However, infection of *Ifnar*$^{-/-}$ BBB cultures yielded lower levels of type I IFNs (Fig. 1E; see Fig. S2A and B in the supplemental material), consistent with a loss of IFNAR-mediated amplification, as well as modestly enhanced TNF-α and more robustly enhanced IL-1β expression (Fig. 1E). Baseline expression of cytokines in uninfected cultures did not differ between genotypes (see Fig. S2), and cytokine expression in bottom culture chambers did not differ substantially from that in top culture chambers (data not shown). These data indicate that type I IFN signaling in BMECs can modulate permeability both directly and indirectly through the suppression of Th1 cytokine expression.

To determine if permeability changes are associated with structural changes involving TJs, BMEC monolayers treated overnight with cytokines, followed by 6 h of WNV infection, were evaluated by immunocytochemistry (ICC) for the TJ proteins Zo-1 and Claudin-5. Infection of WT cells enhanced TJ protein colocalization at intercellular borders, indicating the recruitment and stabilization of these proteins in functional TJ complexes (Fig. 1F and G). In contrast and consistent with TEER responses, infection of *Ifnar*$^{-/-}$ BMECs resulted in decreased TJ protein colocalization, suggesting that type I IFN is necessary to enhance TJ formation in the presence of WNV. Also mirroring our prior TEER results, TNF-α or IL-1β treatment resulted in decreased TJ protein colocalization, which could be rescued by subsequent WNV infection in WT, but not *Ifnar*$^{-/-}$, BMECs. These data indicate that innate

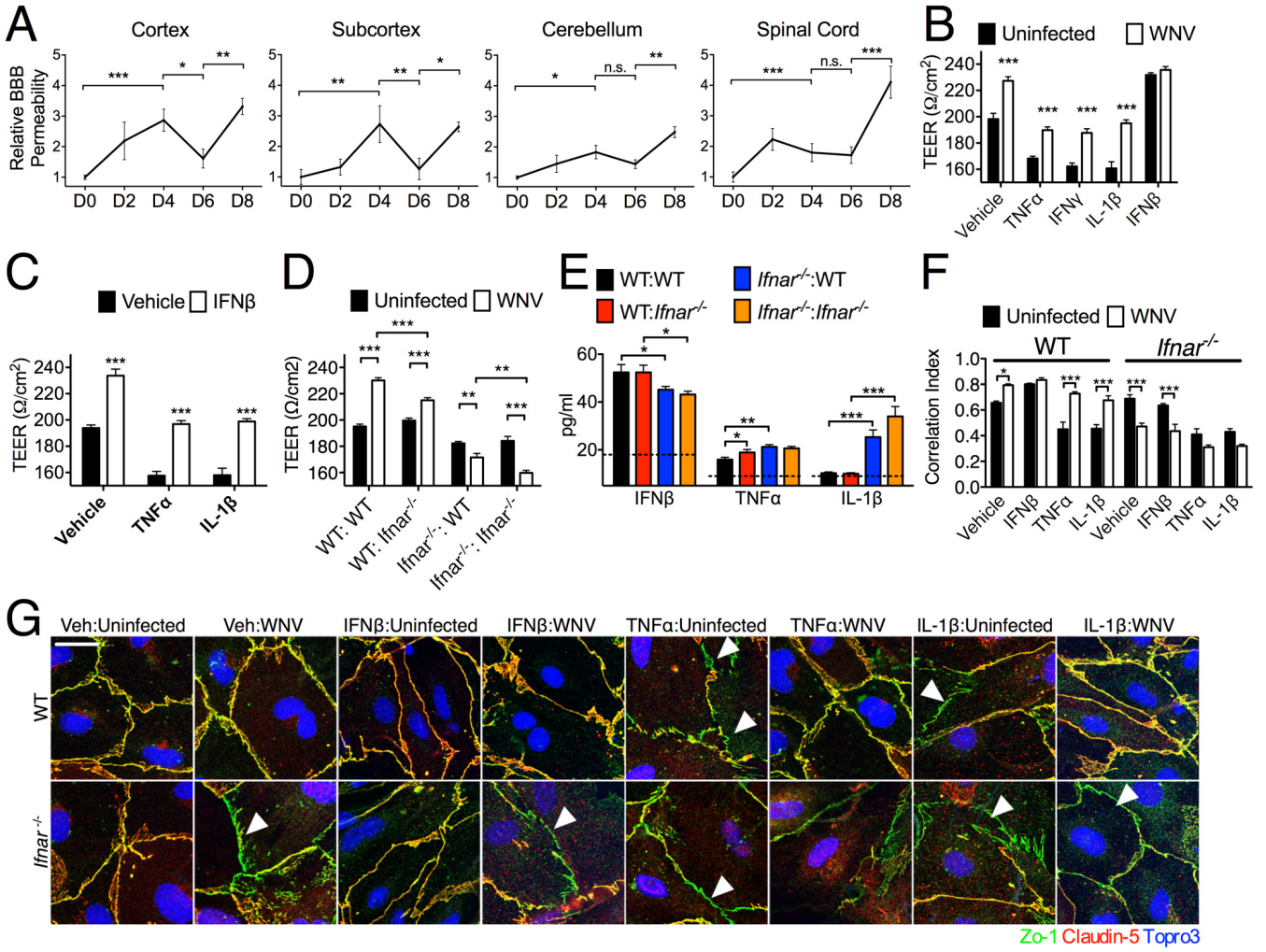

FIG 1 WNV infection modulates endothelial barrier integrity via innate cytokine signaling. (A) Five-week-old C57BL/6 mice were inoculated in the footpad with 100 PFU of WNV and then assessed for BBB sodium fluorescein permeability in CNS regions on the postinfection days indicated. The values reported are arbitrary fluorescence values in CNS tissue normalized to values in serum for individual mice. Group means are normalized to the mean value for uninfected animals. The values on the *x* axes are times in days. n.s., not significant. (B) *In vitro* BBBs were treated overnight in the top chamber with the saline vehicle, TNF-α, IFN-γ, IL-1β, or IFN-β, followed by an additional 6 h of infection with WNV and subsequent measurement of TEER. (C) BBB cultures were treated for 2 h with the vehicle or the cytokine indicated, and then the culture medium was washed away and replaced with medium containing the vehicle or IFN-β for 2 h, followed by measurement of TEER. (D) *In vitro* BBBs were constructed with WT or *Ifnar*$^{-/-}$ BMECs cocultured with astrocytes of either genotype, as shown on the *x* axis, with the BMEC genotype on the left and the astrocyte genotype on the right. TEER measurements after 6 h of WNV infection are shown. (E) ELISA of cytokine expression in the top chambers of BBB cultures following 6 h of WNV infection. (F) Quantification of ICC analysis of colocalization of Zo-1 and Claudin-5 in WT and *Ifnar*$^{-/-}$ BMEC monolayers treated for 2 h with the saline vehicle or the cytokine indicated and subsequently infected for 6 h with WNV at an MOI of 0.01. Values on the *y* axis (correlation indexes) represent the probability of an individual pixel staining positive for both markers if it stains positive for either. (G) Representative ×63 images of cultures with Zo-1 shown in green, Claudin-5 in red, and Topro3 nuclear staining in blue. Scale bar = 25 μm. White arrowheads highlight junctions with loss of TJ protein colocalization. Veh, vehicle.

cytokine signaling in BMECs following exposure to WNV results in the rapid modulation of TJ complexes, which are key regulators of paracellular permeability, and that barrier dysregulation by Th1 cytokines can be controlled by the actions of type I IFN.

PRR activation is sufficient to induce cytokine-dependent changes in endothelial barrier integrity. As type I IFN signaling enhances both TJ formation and BBB permeability after WNV infection, we assessed whether this was the result of classical innate immune signaling through PRRs. First, we inactivated purified WNV via either 2 h of exposure to UV light (WNV-UV) or incubation with 0.1% (vol/vol) β-propiolactone (WNV-BPL), generating viral stocks that are unable to replicate within cells, as assessed via standard plaque assay (data not shown), but do induce the expression of both IFN-β and IFN-α in BMECs after 6 h (see Fig. S2A and B). Treatment of *in vitro* BBB cultures consisting of WT versus *Ifnar*$^{-/-}$ BMECs (both over WT astrocytes) with either WNV-UV or WNV-BPL at an MOI of 0.01 (Fig. 2A) for 6 h revealed enhanced TEER in WT cultures but reduced TEER in *Ifnar*$^{-/-}$ cultures, largely phenocopying the effect of normal virus. These results suggest that type I IFN-dependent changes in TEER require viral detection but not replication in BMECs.

We next determined if direct activation of PRRs was sufficient to alter TEER. TLR3 agonism via 6 h of treatment with naked (nontransfected) poly(I · C) at 1 μg/ml significantly decreased

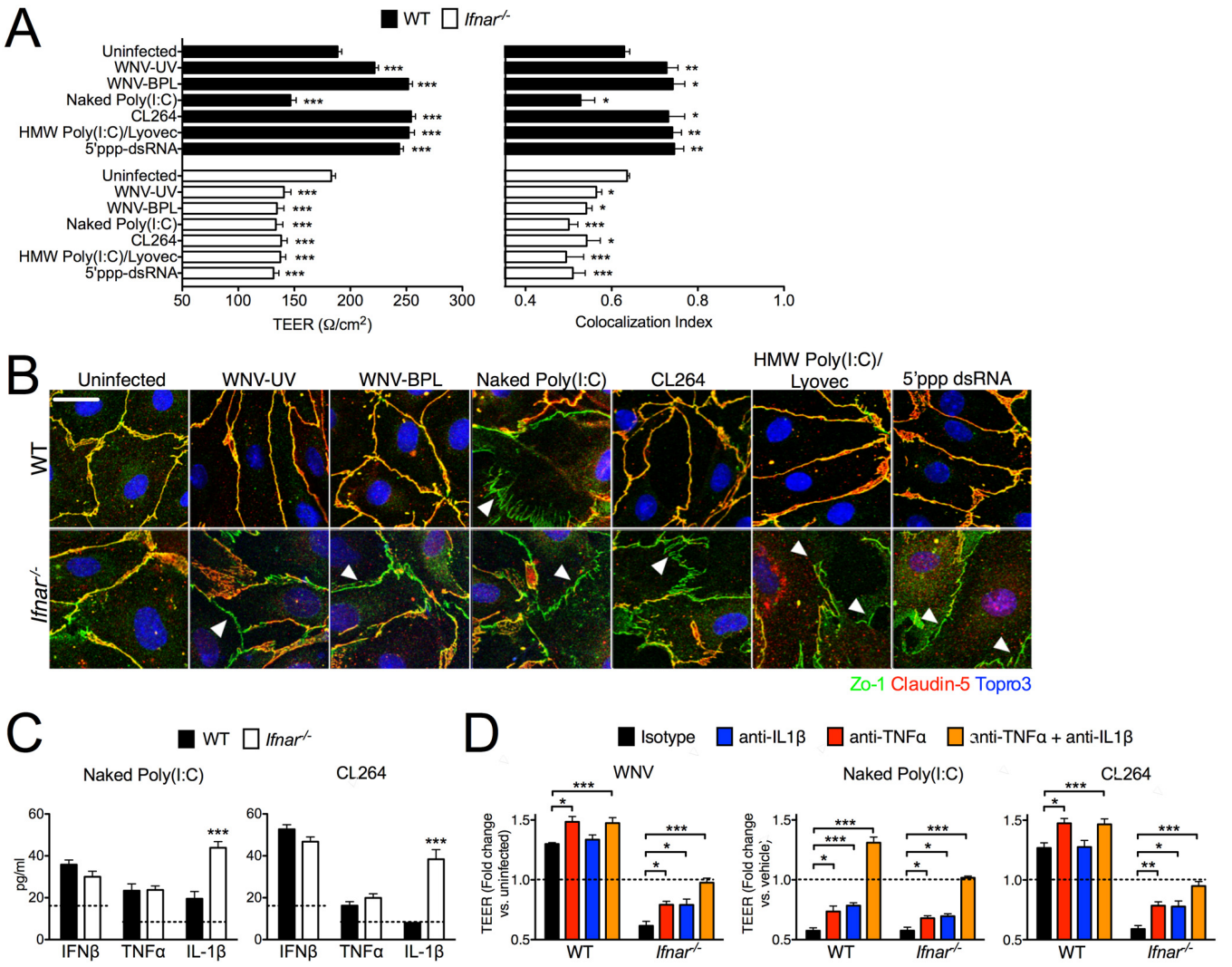

FIG 2 PRR activation is sufficient to induce cytokine-dependent changes in endothelial barrier integrity. (A, left side) TEER measurements for *in vitro* BBBs constructed with either WT or *Ifnar*$^{-/-}$ BMECs over WT astrocytes, treated for 6 h at an MOI of 0.01 with WNV inactivated with UV (WNV-UV), β-propiolactone (WNV-BPL), the TLR3 agonist "naked" poly(I · C), the TLR7 agonist CL264, the MDA5-biased agonist HMW poly(I · C)-LyoVec, or the RIG-I agonist 5′ ppp-dsRNA. (A, right side) Quantification of ICC analysis of colocalization of Zo-1 and Claudin-5 in WT versus *Ifnar*$^{-/-}$ BMECs treated as indicated on the left. Values on the *x* axis (correlation indexes) represent the probability of an individual pixel staining positive for both markers if it stains positive for either. (B) Representative ×63 images showing colocalization of Zo-1 and Claudin-5 in WT versus *Ifnar*$^{-/-}$ BMEC monolayers treated for 6 h with inactivated WNV or a PRR agonist (as in panel A), with Zo-1 shown in green, Claudin-5 in red, and Topro3 nuclear staining in blue. White arrowheads highlight junctions with loss of TJ protein colocalization. (C) ELISA of cytokine production in the top chambers of BBB cultures as in panel A following 6 h of treatment with either "naked" poly(I · C) or CL264. (D) BBB cultures as in panel A were pretreated with neutralizing antibodies to TNF-α and/or IL-1β or isotype controls. Cultures were then infected for 6 h with WNV at an MOI of 0.01 (left panel) or treated for 6 h with "naked" poly(I · C) or CL264 (middle and right panels). Data are expressed as fold changes in infected/treated cultures versus similarly treated mock-infected/vehicle-treated cultures under the same conditions.

TEER in both WT and *Ifnar*$^{-/-}$ BBB cultures (Fig. 2A). However, similar 6-h treatments with agonists for TLR7 (CL264, 10 μg/ml), MDA5 [high-molecular-weight poly(I · C), 1 μg/ml, transfected into cytoplasm], or RIG-I (5′ triphosphate double-stranded RNA [ppp-dsRNA], 1 μg/ml, transfected into cytoplasm) instead resulted in increased TEER in WT cultures but decreased TEER in *Ifnar*$^{-/-}$ cultures, similar to the results obtained with both infectious and inactivated WNV. Enzyme-linked immunosorbent assay (ELISA) results confirmed that the expression of both IFN-β and IFN-α was induced by all of the treatments used, including a TLR3 agonist (see Fig. S2A and B). Consistent with these results, ICC analysis of Zo-1 and Claudin-5 similarly showed enhanced colocalization in WT BMECs treated for 6 h with WNV-UV, WNV-BPL, and TLR7, MDA5, and RIG-I, but not TLR3, agonists, with decreases in TJ protein colocalization after these treatments in *Ifnar*$^{-/-}$ BMECs (Fig. 2A and B). TLR3 agonism, however, resulted in decreases in TJ protein colocalization in both WT and *Ifnar*$^{-/-}$ cultures.

We next assessed if differences in barrier responses to PRR agonists in WT versus *Ifnar*$^{-/-}$ BBB cultures and between TLR3 and other PRR agonists were due to differential cytokine expression. Similar to experiments with WNV, *Ifnar*$^{-/-}$ BBB cultures had small modulations of type I IFN and TNF-α signaling after stimulation with inactivated virus and PRR agonists (see Fig. S2A

to C) and, strikingly, significantly enhanced expression of IL-1β compared to that in WT cultures (see Fig. S2D). Moreover, TLR3 agonism resulted in IL-1β expression even in WT cultures (Fig. 2C), in contrast to cultures treated with other PRR agonists, including the TLR7 agonist CL264, which induced detectable levels of IL-1β only in *Ifnar*$^{-/-}$ BBB cultures (Fig. 2C; see Fig. S2D). To determine if differential expression of Th1 cytokines contributed to differences in TEER responses in BBB cultures exposed to WNV or PRR agonists for 6 h, we measured TEER in the presence of cytokine-neutralizing antibodies. Blockade of TNF-α augmented increases in TEER in WT cultures following exposure to WNV or a TLR7 agonist (Fig. 2D) and partially rescued decreases in TEER in *Ifnar*$^{-/-}$ cultures. In contrast, blockade of IL-1β did not impact TEER in WNV and TLR7 agonist-treated WT cultures, which do not express IL-1β within 6 h, but did partially rescue decreases in TEER in *Ifnar*$^{-/-}$ cultures, which do exhibit IL-1β expression. Similarly, blockade of either TNF-α or IL-1β partially rescued TEER responses in TLR3 agonist-treated cultures of either genotype (Fig. 2D). Of note, simultaneous blockade of both TNF-α and IL-1β in *Ifnar*$^{-/-}$ cultures following exposure to WNV or PRR agonists held TEER levels at baseline values. Together, these data suggest that innate cytokine signaling in BMECs orchestrates barrier responses following exposure to WNV PAMPs and that the relative balance of type I IFN versus TNF-α and IL-1β governs these changes. Type I IFN signaling in BMECs is able to prevent BBB dysregulation by Th1 cytokines, which, in the absence of type I IFN, are able to increase barrier permeability and disassemble TJs. Moreover, PRR activation in BMECs, even in the absence of direct infection, is sufficient to induce cytokine-mediated changes in BBB physiology.

WNV modulates BMEC Rho GTPase signaling in an innate cytokine-dependent manner. To assess the signaling events that regulate BBB physiology downstream of WNV and cytokine signaling, we examined if WNV infection resulted in changes in the activity of Rho GTPases, a family of signaling molecules that regulate cytoskeletal dynamics, including TJs and paracellular permeability (26). WT and *Ifnar*$^{-/-}$ BMEC monolayers were infected for 6 h with WNV, and protein lysates were collected and incubated with Rhotekin or p21-activated protein kinase (PAK) agarose beads to pull down GTP-bound, activated Rac1, RhoA, and CDC42. Western blot detection of activated forms of these GTPases revealed a significant increase in activated Rac1 in WNV-infected WT BMECs (Fig. 3A and B) and a significantly smaller increase in activated Rac1 in *Ifnar*$^{-/-}$ BMECs. In contrast, while activated RhoA was not increased in WNV-infected WT BMECs, *Ifnar*$^{-/-}$ BMECs exhibited significantly increased amounts of activated RhoA (Fig. 3A and C). Levels of activated CDC42 were not affected by WNV infection in either WT or *Ifnar*$^{-/-}$ BMEC cultures (Fig. 3A and D). As these experiments suggested a dynamic range of Rho GTPase activation responses following WNV infection, we next assessed the manner in which individual innate cytokines regulate Rho GTPase activation. In agreement with infection experiments with WT versus *Ifnar*$^{-/-}$ BMECs, 2 h of incubation of WT BMECs with recombinant IFN-β resulted in significantly enhanced Rac1 activation (Fig. 3E and F) and significantly diminished RhoA activation (Fig. 3E and G). In contrast, 2 h of incubation with TNF-α resulted in decreased Rac1 activation and greater activation of RhoA, while 2 h of IL-1β treatment increased the activation of both GTPases, with a greater fold change in induction of RhoA activation.

Innate cytokine-dependent modulation of Rac1 and RhoA after WNV infection regulates BBB permeability and TJ formation. We next examined whether modulation of BMEC Rho GTPase signaling in the context of WNV infection contributes to type I IFN-dependent regulation of TEER and TJ responses. Pharmacological blockade of Rac1 signaling via 2 h of pretreatment with its specific inhibitor, Z62954982, abolished the increase in TEER after 6 h of WNV infection in WT cells, with TEER values significantly decreased in WNV-infected WT barriers in the absence of Rac1 signaling, while responses remain unchanged in similarly infected and treated *Ifnar*$^{-/-}$ barriers (Fig. 3H). Conversely, inhibition of RhoA signaling via 2 h of pretreatment with its specific inhibitor, H1152P, did not impact TEER changes induced by WNV infection in WT barriers but significantly rescued reductions in TEER in similarly infected and treated *Ifnar*$^{-/-}$ barriers. Inhibition of CDC42 via 2 h of pretreatment with ML141, a specific inhibitor of CDC42, did not significantly alter TEER in either WT or *Ifnar*$^{-/-}$ barriers after WNV infection. As changes in TEER responses could simply be explained by altered IFN expression by BMECs following infection in the presence of GTPase inhibitors, we confirmed via ELISA that inhibition of Rac1 or RhoA did not significantly alter IFN-β levels in luminal chambers following 6 h of infection and that none of the inhibitors impacted TEER in cultures mock infected for 6 h (see Fig. S3A to C in the supplemental material).

Consistent with analyses of TEER, ICC analysis further revealed that inhibition of Rac1 signaling in WT cells completely abolished the increase in the colocalization of Zo-1 and Claudin-5 observed in WNV-infected WT BMECs (Fig. 3I and J), while inhibition of RhoA or CDC42 did not impact TJ formation in WT cells. However, inhibition of RhoA rescues the loss of TJ formation in WNV-infected *Ifnar*$^{-/-}$ BMECs, abolishing decreases in TJ protein colocalization observed in untreated *Ifnar*$^{-/-}$ BMECs. Inhibition of Rac1 or CDC42 did not significantly impact TJ formation in *Ifnar*$^{-/-}$ BMECs. Control experiments also confirmed that 2 h of pretreatment with GTPase inhibitors, followed by 6 h of mock infection, did not change baseline levels of TJ protein colocalization (see Fig. S3D). Together, these data suggest that cytokines expressed in BMECs following exposure to WNV differentially influence Rho GTPase activity, with type I IFN contributing to the preferential activation of Rac1, thereby stabilizing barrier physiology. This regulation counteracts the activity of the cytokines TNF-α and IL-1β, which preferentially activate RhoA and contribute to barrier disruption.

Innate cytokine regulation of Rho GTPase signaling controls WNV transmigration across the *in vitro* BBB. We next determined if cytokine and Rho GTPase modulation of TEER and TJ integrity are relevant regulators of viral trafficking across the BBB, limiting the access of WNV to the CNS. For these experiments, WNV at an MOI of 0.01 was added to the top chamber of Transwell BBB cultures; 6 h later, the top chamber was removed, such that only virus that had crossed during the 6 h of incubation was present in the bottom chamber. Amounts of migrated virus in the bottom chambers were then assessed via multistep growth curve analysis. Consistent with changes in TEER and TJ integrity, overnight pretreatment of the top chamber with TNF-α or IL-1β before infection significantly enhanced the transendothelial migration of WNV (Fig. 4A and B), while IFN-β pretreatment of the top chamber significantly reduced viral trafficking (Fig. 4C). Similarly, experiments with barriers with WT versus *Ifnar*$^{-/-}$ BMECs

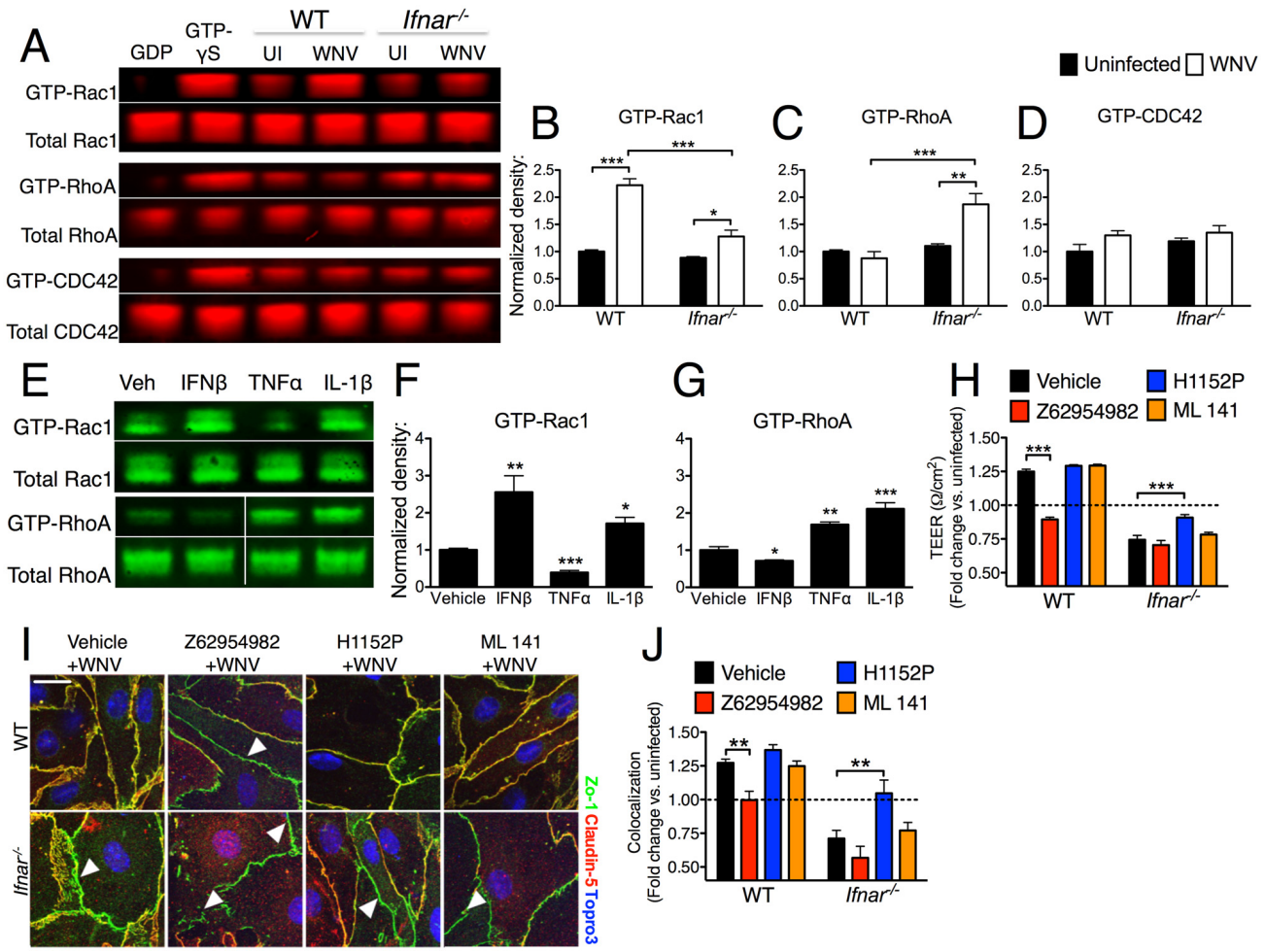

FIG 3 WNV modulates endothelial Rho GTPase-mediated regulation of the BBB endothelium. (A to G) Activated GTPase pulldown assay of WT or *Ifnar*$^{-/-}$ BMECs either infected with WNV at an MOI of 0.01 for 6 h (A to D) or treated for 2 h with recombinant TNF-α, IL-1β, or IFN-β (E to G). After treatment, BMEC lysates were incubated with Rhotekin or PAK agarose beads to purify GTP-bound, activated Rac1, RhoA, and CDC42. Both purified activated GTPases and total unpurified cell lysates were then probed via Western blot assay to assess activated versus total amounts of each GTPase. UI, uninfected. (B to D, F, G) Density quantification of activated Rac1 (B, F), RhoA (C, G), or CDC42 (D), normalized to the total amount of each protein in each sample. Group averages are normalized to the mean values of uninfected/vehicle-treated WT BMECs. (H) TEER measurements for *in vitro* BBBs constructed with WT or *Ifnar*$^{-/-}$ BMECs over WT astrocytes, pretreated for 2 h with Rac1 inhibitor Z62954982, ROCK/RhoA inhibitor H1152P, or CDC42 inhibitor ML141 and then infected for 6 h with WNV at an MOI of 0.01. Data are reported as fold changes in TEER in infected cultures versus uninfected cultures within each treatment group. (I) Representative ×63 images showing colocalization of Zo-1 and Claudin-5 in WT versus *Ifnar*$^{-/-}$ BMEC monolayers treated for 2 h with GTPase inhibitors (as in panel H), followed by 6 h of infection with WNV at an MOI of 0.01, with Zo-1 shown in green, Claudin-5 in red, and Topro3 nuclear staining in blue. White arrowheads highlight junctions with loss of TJ protein colocalization. (J) Quantification of colocalization in images in panel I. Data are reported as the fold changes in colocalization in infected cells versus uninfected cells within each treatment group.

over WT astrocytes revealed that *Ifnar*$^{-/-}$ BMECs exhibit significantly enhanced viral migration (Fig. 4D). In order to control for the possibility that IFN-β treatment or genetic deletion of IFNAR on BMECs alters the basolateral secretion of type I IFN by BMECs, which may skew the kinetics of replication in the astrocytes below, we did concurrent experiments with BBB cultures with *Ifnar*$^{-/-}$ astrocytes. These experiments yielded similar results, confirming that differential exposure of astrocytes to IFN did not account for the difference observed in experiments with WT astrocytes (see Fig. S4A and B in the supplemental material). Pretreatment of BBB cultures with neutralizing antibodies to TNF-α reduced viral migration in both WT *Ifnar*$^{-/-}$ cultures, while pretreatment with neutralizing antibodies to IL-1β reduced migration only in *Ifnar*$^{-/-}$ cultures, consistent with similar experiments measuring TEER responses (Fig. 4E and F). Once again, neutralizing antibodies to both cytokines had additive effects on *Ifnar*$^{-/-}$ barriers, suppressing viral migration back to the levels observed in WT cultures.

As cytokine signaling was observed to influence transendothelial viral migration, we next performed similar experiments in which cultures consisting of WT or *Ifnar*$^{-/-}$ BMECs over WT astrocytes were pretreated for 2 h in the top chamber with antagonists of Rac1, RhoA, or CDC42 prior to the introduction of WNV. Again, consistent with TEER and TJ integrity findings, antagonism of Rac1 significantly enhanced the transendothelial migration of WNV across WT BMECs but did not further augment the enhanced migration observed across *Ifnar*$^{-/-}$ BMECs (Fig. 4G). Likewise, antagonism of RhoA did not significantly alter

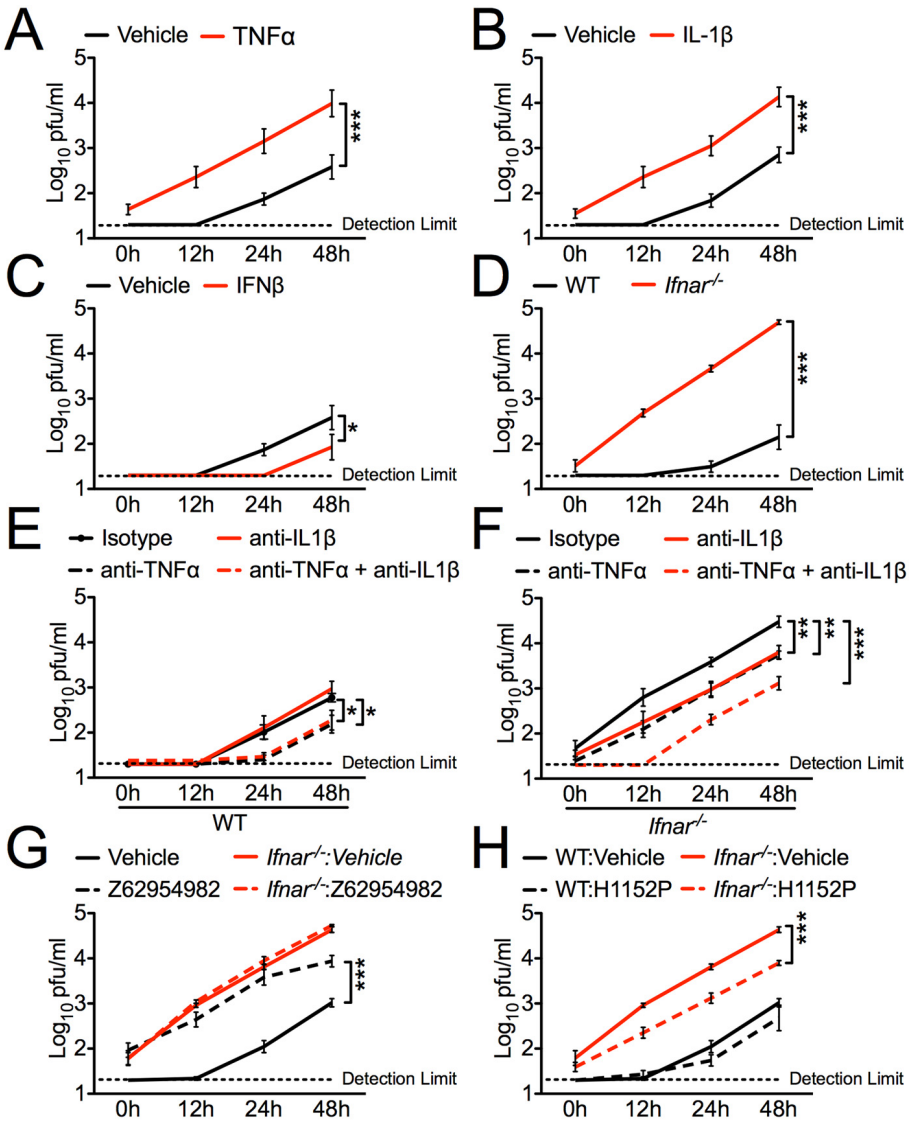

FIG 4 Innate cytokines differentially regulate WNV transmigration across the *in vitro* BBB. (A to H) Detection of replicating virus in the bottom chambers of *in vitro* BBBs constructed with the WT BMECs only (A to C) or WT or *Ifnar*$^{-/-}$ BMECs (D to H) over WT astrocytes, infected with WNV at an MOI of 0.01 in the top chambers for 6 h before removal of the top chambers. The cultures in panels A to C were treated overnight with the saline vehicle or TNF-α (A), IL-1β (B), or IFN-β (C) prior to infection. The cultures in panels E and F were pretreated for 2 h with neutralizing antibodies to TNF-α (E) or IL-1β (F) before infection. The cultures in panels G and H were pretreated for 2 h with Rac1 inhibitor Z62954982 (G) or ROCK inhibitor H1152P (H) before infection. Values are viral titers present after 0, 12, 24, and 48 h of replication by virus that crossed during the 6 h of infection, prior to the removal of BMECs from the culture system. Viral titers are reported in plaque-forming units per milliliter, as determined via standard plaque assay in BHK cells. Each horizontal dotted line represents the limit of detection of the assay.

WNV migration across WT BMECs but resulted in a partial rescue of the enhanced migration observed in *Ifnar*$^{-/-}$ BMECs (Fig. 4H). As expected antagonism of CDC42 did not impact the transendothelial migration of WNV (see Fig. S4C). Together, these findings suggest that modulation of BMEC TEER and TJs caused by type I IFN-dependent regulation of Rho GTPases is consequential to the ability of WNV to traffic across the BBB endothelium.

Mice with impaired type I IFN responses exhibit enhanced BBB permeability and loss of TJ integrity after peripheral WNV infection. Mice lacking a type I IFN receptor, ligands, and regulatory transcription factors exhibit enhanced susceptibility to WNV infection, including early entry of virus into the CNS compared to WT controls. Thus, in light of our *in vitro* observations, we wondered if mice with impaired type I IFN signaling would also exhibit alterations in BBB permeability and TJ integrity following peripheral infection. To determine whether type I IFN signaling is required for the *in vivo* decrease in BBB permeability observed on day 6 after WNV infection of the CNS, we examined BBB permeability in the context of i.c. inoculation (10 PFU) of WNV in 8-week-old WT versus *Ifnar*$^{-/-}$ mice. WT animals experienced a significant decrease in BBB permeability to sodium fluorescein on days 1 and 2 in each CNS region, followed by a large increase in BBB permeability on day 4 (Fig. 5A), coincident with the detection of large numbers of inflammatory cells at this time point in this model (27). However, these kinetics were not observed in *Ifnar*$^{-/-}$ animals, which instead exhibited a significant and sustained in-

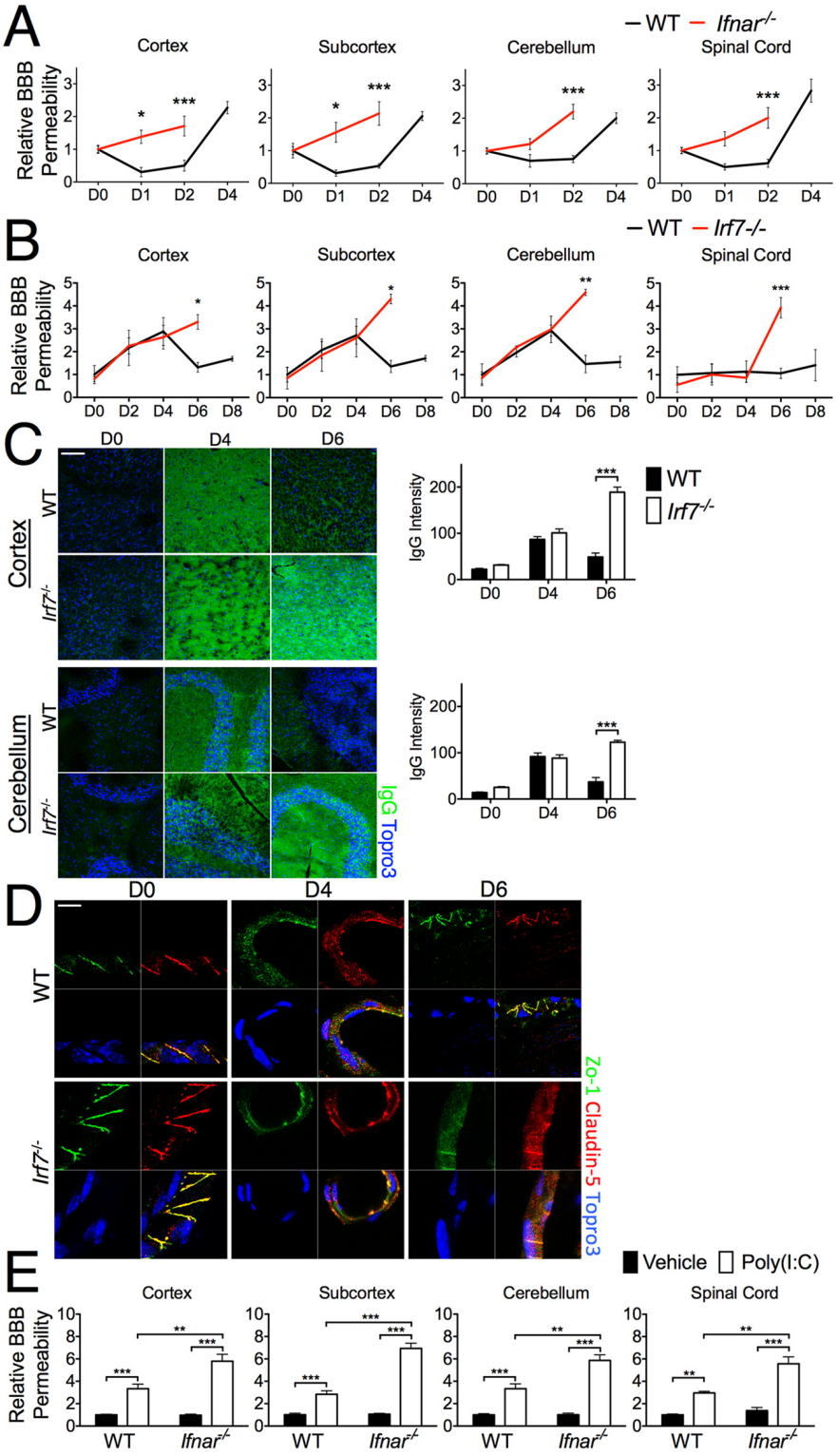

FIG 5 WT mice but not mice with impaired type I IFN signaling exhibit increased BBB integrity following neuroinvasion. (A) Eight-week-old WT and *Ifnar*$^{-/-}$ mice were i.c. inoculated with 10 PFU WNV. On the days indicated after infection, mice were administered sodium fluorescein and then sodium fluorescein levels in tissue homogenates taken from CNS regions contralateral to the inoculation site were assessed. The values reported are arbitrary tissue fluorescence values normalized to the serum values of individual mice. Group means are normalized to the mean value of mock-infected WT animals. (B) Sodium fluorescein permeability in CNS regions after footpad inoculation with 100 PFU WNV. Values taken from CNS regions (both hemispheres) are reported as in panel A, with normalization to values of uninfected WT mice. (C) IHC detection of serum IgG in parenchymal CNS tissues after peripheral WNV infection, with quantification of group mean fluorescence intensity per low-power field. Scale bar = 100 μm. (D) IHC detection of Zo-1 (green) and Claudin-5 (red) in CNS microvessels on the days after footpad infection indicated. Scale bar = 10 μm. (E) Eight-week-old WT and *Ifnar*$^{-/-}$ mice were administered 50 μg poly(I · C) i.p., followed by sodium fluorescein 24 h later (processed as described for panel B).

crease in permeability to sodium fluorescein each day following infection. For these studies, we examined permeability in tissues contralateral to the inoculation site, though we ultimately found that permeability did not differ significantly between hemispheres on any day following i.c. infection (data not shown). Concurrent experiments with mice that received mock i.c. inoculations with saline showed only extremely modest increases in BBB permeability, which did not differ between WT and *Ifnar*$^{-/-}$ mice (see Fig. S5 in the supplemental material); thus, the inoculation procedure alone did not explain changes in BBB permeability following i.c. inoculation with WNV. In all, these data suggest that local type I IFN responses in the CNS following WNV entry promote BBB integrity, which may contribute to the decrease in BBB permeability observed between days 4 and 6 following peripheral infection.

As *Ifnar*$^{-/-}$ mice rapidly and uniformly die of septic shock (at about 3.5 days after footpad infection) (16, 28), we next used *Irf7*$^{-/-}$ mice, which have impaired expression of IFN-α (29). These mice experience early neuroinvasion of WNV compared to WT mice following footpad infection (29). Sodium fluorescein permeability experiments revealed that WNV-infected 8-week-old WT mice exhibit BBB permeability kinetics similar to those previously observed in 5-week-old animals, including an increase in permeability during peripheral infection (days 0 to 4), followed by a decrease in permeability at day 6 (Fig. 5B). In contrast, WNV-infected 8-week-old *Irf7*$^{-/-}$ mice exhibit a sustained increase in BBB permeability over the entire course of infection, with significantly higher permeability than that of WT controls on day 6. Immunohistochemical (IHC) detection of extravasated endogenous IgG revealed similar kinetics of permeability following WNV infection in cortical and cerebellar tissues (Fig. 5C). Consistent with this, IHC detection of Zo-1 and Claudin-5 in CNS tissues revealed that both WT and *Irf7*$^{-/-}$ mice exhibited loss of TJ integrity on day 4 following WNV infection, characterized by diminished or diffuse cytoplasmic staining of TJ proteins and substantially decreased colocalization of TJ proteins at cell-cell borders (Fig. 5D). Alteration in TJ assembly was reversed at day 6 within the microvasculature of WNV-infected WT mice, while that of similarly infected *Irf7*$^{-/-}$ mice showed sustained dysregulation of TJs. As differences between the viral burdens of WT and *Irf7*$^{-/-}$ mice over time complicate the interpretation of BBB changes due to type I IFN signaling, we performed control experiments in which WT and *Ifnar*$^{-/-}$ mice were treated with the TLR3 agonist poly(I · C), which is known to increase BBB permeability (6). At 24 h following treatment, *Ifnar*$^{-/-}$ mice exhibited greater CNS permeability to sodium fluorescein than WT mice (Fig. 5E), providing further evidence that type I IFN signaling is required to preserve BBB integrity in the context of systemic inflammatory activation.

DISCUSSION

While the contributions of innate cytokine responses to virologic control and adaptive immunity during WNV infection are known, the regulatory potential of these molecules at the BBB remains poorly understood. Here, we demonstrate that PRR activation in the presence of WNV in the BBB endothelium results in cytokine-dependent modulation of Rho GTPase signaling, exerting regulatory control over BBB permeability and TJ integrity. This, in turn, is consequential for the ability of WNV to traffic across the BBB endothelium. In particular, our data suggest that the induction of type I IFN serves to preserve and stabilize BBB structure and function both directly and indirectly by limiting barrier disruption caused by the cytokines TNF-α and IL-1β. *In vivo*, BBB permeability increases during peripheral infection but sharply decreases coincident with viral neuroinvasion in WT animals but not in animals with attenuated type I IFN responses, suggesting that local CNS type I IFN responses may act on the BBB to mitigate the access of WNV to the CNS parenchyma.

The Th1 cytokines TNF-α and IL-1β have previously been shown to disrupt barrier endothelium *in vitro* and *in vivo*, increasing permeability (30–32) and dysregulating junction complexes (1, 33, 34). During viral infections, TNF-α, in particular, has been linked to enhanced vascular permeability, poor tissue perfusion, and endothelial cell death (28, 35). Here, we show that TNF-α signaling in BMECs activates RhoA, disrupting barrier function and increasing the transendothelial movement of WNV. This is in line with the study of Wang et al. (6), who reported a decrease in BBB permeability in *Tnfrsf1a*$^{-/-}$ mice following WNV infection. These findings together indicate that Th1 cytokine-mediated disruption of the BBB provides an access route for neuroinvasion by WNV.

In contrast to Th1 cytokines, type I IFN treatment has been established to promote BBB function (34, 36). However, for the first time, we demonstrate that *in vivo* induction of type I IFN following WNV infection is a key regulator of BBB permeability and TJ integrity. Type I IFN signaling in BMECs *in vitro* is shown to enhance barrier function over baseline conditions and to rescue Th1 cytokine-mediated barrier dysregulation, suggesting that CNS type I IFN responses may be able to reverse the BBB permeability caused by Th1 cytokine production during infection *in vivo*. This interpretation agrees with *in vitro* observations suggesting that dengue virus activation of type I IFNs reduces vascular leakage in peripheral endothelium, even in the presence of the barrier-disrupting cytokines (35). Type I IFN also preserves barrier integrity by suppression of Th1 cytokine expression, most noticeably, that of IL-1β. While the interactions of type I IFN and IL-1β during WNV infection vary across tissues and times after infection (12, 13), type I IFN has been shown to suppress IL-1β expression via mechanisms that vary by cell type and inflammatory stimulus, including inhibition of inflammasome activity and pro-IL-1α and pro-IL-1β expression (37, 38). To our knowledge, we are the first to demonstrate IFN-mediated suppression of endogenous IL-1β in the BBB endothelium. While this report and others have identified a role for IL-1 signaling in BBB breakdown (39, 40), we note our previous study showing that IL-1 signaling at the BBB is an important facilitator of lymphocyte activation and trafficking into the CNS during WNV infection and was crucial for viral clearance and survival (13). Moreover, Ramos et al. (12) found that type I IFNs and IL-1β worked synergistically to control WNV in neurons. Thus, IL-1 signaling during WNV infection may serve both pathological and protective functions, and the modulation of these effects by type I IFN likely varies over time and by cell type.

Some studies of murine WNV encephalitis have reported a sustained increase in BBB permeability over the course of infection, with permeability rising coincident with neuroinvasion and continuing to increase thereafter (41, 42). However, our findings more closely resemble those showing markedly enhanced BBB permeability 3 to 4 days postinfection, prior to neuroinvasion (6, 43, 44). Wang et al. (6) additionally observed reduced BBB per-

meability on day 5 postinfection, coincident with neuroinvasion, in concordance with our findings. A similar biphasic response in BBB permeability was also observed in a model of Venezuelan equine encephalitis virus infection (45). The reasons for these discrepancies are unclear and may include variations in the viral inoculation site and the age of the experimental animals used. Nevertheless, our data suggest that type I IFN suppresses BBB permeability during viral infection, as loss of intact type I IFN signaling enhanced BBB permeability following both peripheral and CNS WNV inoculations. While tissue viral burden and immune activation differences between *Ifnar*$^{-/-}$ and *Irf7*$^{-/-}$ mice after peripheral infection may independently contribute to the observed differences in BBB permeability, we note that, following i.c. inoculation, BBB permeability was demonstrated to be significantly higher in *Ifnar*$^{-/-}$ animals, even 1 day after infection when CNS viral titers have been shown to be equivalent (16).

Cytokine-mediated regulation of the BBB is likely to arise from many diverse sources, including peripheral/serum cytokines, CNS cytokines produced by resident and infiltrating cells, as well as cytokines produced by the BBB endothelium that signal in an autocrine or paracrine fashion among BMECs. Here, we have focused our investigation specifically on BMEC-intrinsic cytokine signals, though our data and previous studies provide some clues as to how cytokine signaling from each of these sources may orchestrate the observed changes in BBB permeability. *In vivo* BBB permeability seems to peak initially at day 4 postinfection, most likely because of the actions of Th1 cytokines that accumulate in serum during peripheral infection (13, 46). After viral neuroinvasion, type I IFN is rapidly produced in the CNS, appearing as early as day 5 postinfection (16), while Th1 cytokines are generally not expressed in significant amounts until day 7 or 8 (12, 13, 47). Thus, the initial interaction of the virus with the BBB endothelium and early IFN production within the infected CNS on days 5 and 6 likely function together to produce a decrease in BBB permeability. Increases in inflammatory cytokine levels during later stages of CNS infection derive from both innate immune responses of CNS cells and infiltrating leukocytes expressing TNF-α and IFN-γ, which also are first detectable in significant quantities 7 to 8 days postinfection (47–49). Likewise, following i.c. inoculation, type I IFNs are induced within 2 days (29) as BBB permeability decreases, followed by the infiltration of inflammatory cells on day 4 (27) and a subsequent increase in BBB permeability. Ultimately, the exact timing of the expression and interaction of IFNs and inflammatory cytokines expressed in various compartments following WNV infection is complex and, as in studies of BBB permeability, sometimes differ among reports. However, on the basis of our findings and the general trends observed in the literature, it appears that systemic immune factors contribute to BBB breakdown during peripheral infection, which may contribute to WNV entry into the CNS. Around the time of CNS neuroinvasion, direct interaction of the virus with the BBB endothelium and early, local innate immune responses in the CNS lead to a type I IFN-dependent decrease in BBB permeability, which may be reversed by infiltration of the CNS by inflammatory cells.

Cytokine-mediated BBB regulation is shown to occur via PRR pathways, independently of viral replication, as detection of viral PAMPs in BMECs was sufficient for the regulation of barrier physiology. In particular, agonism of WNV-sensing PRRs RIG-I, MDA-5, and TLR7 induced cytokine responses dominated by type I IFN, thereby enhancing barrier function. Prior studies have revealed that deficiencies in each of these pathways result in increased disease susceptibility, including early neuroinvasion and greater CNS viral burdens during WNV infection (27, 50, 51). Of note, unlike other PRRs, TLR3 agonism increased barrier dysregulation in both WT and *Ifnar*$^{-/-}$ BMECs. Compared to other PRRs, TLR3 induced cytokine responses more heavily skewed toward Th1 cytokines and, uniquely, stimulated rapid expression of IL-1β, even in WT cells. These data align with a previous report (6) suggesting that TLR3 activation contributed to BBB breakdown and subsequent WNV neuroinvasion. In our study, *in vivo* TLR3 agonism also induced BBB permeability and did so more efficiently in *Ifnar*$^{-/-}$ than WT mice, again suggesting that type I IFN expression may counterregulate the effects of TNF-α and IL-1β at the BBB. The specific role of TLR3 during WNV encephalitis remains uncertain, as another report (3) was unable to link TLR3 activation to BBB breakdown. Ultimately, TLR3 signals through an adaptor different from that used by other PRRs (52) and thus may exhibit different regulatory properties at the BBB, as has been shown in other tissues (53). As demonstrated by Verma et al. (2), we found that WNV is capable of trafficking across the BBB endothelium *in vitro*, though this study used high MOIs over several days, leading to increased virus in bottom chambers because of replication within endothelium, independently of paracellular permeability. Alternatively, we show that the virus can cross the BBB endothelium quickly after exposure, independently of replication, and that trafficking is correlated with paracellular permeability. Movement of virus in this manner is likely relevant *in vivo*, as studies have linked host factors that contribute to BBB disruption to WNV neuroinvasion (44, 54, 55). We also demonstrate a rapid (<6 h), cytokine-dependent regulation of TJ protein localization after infection. Type I IFN regulation of BMEC TJs was due to the activation of Rac1 and suppression of RhoA activity, a regulatory regimen well known to control TJ integrity (26). This finding is in line with a report demonstrating that RhoA contributed to the dysregulation of BMEC TJs, enhancing the trafficking of HIV-1-infected monocytes across the BBB (56). Thus, regulation of this pathway may serve to limit CNS trafficking of both free and cell-associated WNV.

Understanding how viral and host factors contribute to the development of neuroinvasive disease is a critical step in developing treatment and prevention strategies for WNV encephalitis. IFN therapy has been used with some success in immunocompetent patients with WNV encephalitis (57, 58), while IFN therapy in immunosuppressed patients, such as recipients of infected transplant organs, has been less successful, according to case reports (59). A limitation of the human treatment literature, however, is that patients have typically developed neuroinvasive disease before treatment; this caveat, combined with the broad systemic effects of IFN therapy, limits our understanding of how IFN may regulate BBB function in human patients. A more promising line of investigation includes the identification of genetic differences in innate immune pathways that may influence disease susceptibility to encephalitis-causing viruses. Studies thus far have associated polymorphisms in several type I IFN pathway elements, including *IRF3*, *MX1*, and *OAS1*, with susceptibility to symptomatic WNV infection (60, 61). In addition, enhanced TLR3 activity and inflammatory cytokine production after WNV infection have been shown in macrophages obtained from elderly patients compared to those of young controls, which may contribute to the enhanced susceptibility of older individuals to neuroinvasive dis-

ease (62). Thus, understanding how variations in innate immune factors contribute to susceptibility to viral encephalitis may inform new strategies for prevention and targeted therapeutics.

MATERIALS AND METHODS

Murine model of WNV encephalitis. Five- and 8-week-old C57BL/6 mice were commercially obtained (Jackson Laboratories). Congenic *Ifnar*$^{-/-}$ and *Irf7*$^{-/-}$ mice were the generous gift of Michael Diamond (Washington University in St. Louis). All animals were housed under pathogen-free conditions in the animal facilities of the Washington University School of Medicine. All experiments were performed in compliance with Washington University animal studies guidelines. Mice were inoculated subcutaneously via footpad injection (50 μl) or i.c. (2 μl) with either 100 or 10 PFU of WNV, respectively, as previously described (23). WNV strain 3000.0259 (isolated in New York in 2000 [63]) was used in all experiments. Viral titers in all experiments were determined via standard plaque assay in BHK21-15 cells as previously described (64).

***In vivo* assessment of BBB permeability.** At various day intervals after infection, mice were injected i.p. with 100 μl of 100 mg/ml fluorescein sodium salt (Sigma-Aldrich) in sterile phosphate-buffered saline (PBS). After 45 min, mice underwent extensive cardiac perfusion with PBS, followed by collection of blood and harvesting of CNS tissues. Tissue homogenates and serum were incubated overnight at 4°C at a 1:1 dilution in 2% trichloroacetic acid (Sigma-Aldrich) to precipitate protein, which was pelleted by 10 min of centrifugation at 4,000 rpm at 4°C. Supernatants were then diluted in equal volumes of borate buffer, pH 11 (Sigma-Aldrich). Fluorescence emission at 538 nm was determined via a Synergy H1 microplate reader and Gen5 software (BioTek Instruments, Inc.). Tissue fluorescence values were standardized against plasma values for individual mice.

***In vitro* BBB cultures and TEER recordings.** Primary murine BMECs were prepared from 8- to 10-week-old WT and *Ifnar*$^{-/-}$ mice as previously described (65). Primary neonatal murine astrocytes were prepared from WT and *Ifnar*$^{-/-}$ pups (postnatal days 1 to 3) from mixed glial cultures as previously described (66). *In vitro* BBB cultures were then prepared as previously described (67). Briefly, 10^5 BMECs were cultured on the apical side of a 0.9-cm^2 fibronectin-coated polyethylene terephthalate filter insert with a 3.0-μm pore size (BD Falcon). A total of 10^5 astrocytes were cultured concurrently in 12-well plates until they reached confluence (~2 days), at which point BMEC inserts were added to astrocyte cultures. Resistance recordings were made via chopstick electrode with an EVOM voltmeter (World Precision Instruments). Resistance values are reported in Ω/cm^2 (recorded values minus values for cell-free inserts).

ICC and IHC analyses. ICC analysis on primary BMECs was performed after 10 min of fixation in ice-cold methanol, followed by blocking for 30 min in 10% goat serum in PBS at room temperature (RT). Cells were then incubated with primary antibodies to Zo-1 (rat anti-mouse monoclonal antibody, clone R40.76; Millipore) and Claudin-5 (rabbit anti-mouse polyclonal antibody; Invitrogen) in blocking buffer for 1 h at RT, washed three times in PBS, and then incubated for 15 min in goat anti-rat Alexa Fluor 488-conjugated and goat anti-rabbit Alexa Fluor 555-conjugated secondary antibodies in blocking buffer at RT. CNS tissue sections were obtained from WT and *Irf7*$^{-/-}$ mice after cardiac perfusion with 4% paraformaldehyde. Tissues were frozen, blocked, and stained with the primary and secondary antibodies listed above as previously described (47). Nuclei in all preparations were stained with Topro3. All images were acquired via confocal microscopy (Carl Zeiss USA). Colocalization statistics were obtained via analysis with ImageJ software.

ELISA. Sandwich ELISA kits were used for detection of cytokine levels in cell culture supernatants. ELISA kits for IFN-β and IFN-α (PBL InterferonSource), TNF-α (EBioscience), and IL-1B (R&D Systems) were used according to the manufacturers' instructions. Colorimetric reading of ELISA plates was performed with a Synergy H1 microplate reader and Gen5 software (BioTek Instruments, Inc.).

Virus inactivation. Stocks of WNV (NY-2000, 2×10^4 PFU/ml) were incubated in 0.1% (vol/vol) β-propiolactone (Sigma) for 30 min at 4°C. BPL in viral stocks was then inactivated by incubating the stocks for 2 h at 37°C, followed by hydrolysis of BPL via subsequent overnight incubation at 4°C. Alternatively, similar stocks were placed in 35-mm^2 culture plates and incubated in a dark chamber above a UV transilluminator box (Stratagene) for 2 h at RT. Inactivated viral stocks were stored at −80°C.

Neutralizing-antibody studies. Neutralizing-antibody studies were performed after 2 h of pretreatment with purified anti-mouse TNF-α (1 μg/ml, clone TN3-19; EBioscience) and anti-mouse IL-1β (1 μg/ml, clone B122; Leinco) antibodies. IgG isotype antibodies were used as negative controls.

GTPase studies. GTPase pulldown experiments were performed with an activated Rac1/RhoA/CDC42 Rhotekin and PAK agarose bead kit (Cell BioLabs, Inc.) according to the manufacturer's instructions. Purified, GTP-bound protein and unpurified BMEC protein lysates were separated via gel electrophoresis on 10% bis-Tris gels (Invitrogen) and transferred onto iBlot nitrocellulose transfer membranes (Invitrogen) according to standard protocols. Blots were probed with primary antibodies against Rac1, RhoA, and CDC42 (Cell Biolabs), followed by incubation with IRDye-conjugated secondary antibodies (LI-COR). Blots were imaged with the Odyssey fluorescent scanning system (LI-COR). TEER and viral trafficking experiments involving inhibition of GTPase signaling were performed as previously described (68), with *in vitro* BBBs after 2 h of pretreatment in the top chamber at 37°C with the following agents: the Rac1 inhibitor Z62954982 (1 mM; Cayman Chemical Co.), the Rho/ROCK inhibitor H-1152P (10 nM; Cayman Chemical Co.), and the CDC42 inhibitor ML141 (100 nM; Tocris-R&D Systems).

Statistical analysis. All of the data reported here are mean values ± the standard errors of the means. Data reported for *in vitro* TEER and cytokine expression experiments include 6 to 12 replicates from two or three independent experiments. *In vitro* ICC analyses include five or six replicates from two independent experiments. *In vivo* fluorescein experiments included six mice/group/day from two independent experiments. *In vivo* IHC analyses included five mice/group/day from two independent experiments. All group effects were compared via one- or two-way analysis of variance; Bonferroni's *post hoc* test was subsequently used to compare individual means. Correction for repeated measures was also used where appropriate. All statistical analysis was performed with GraphPad Prism software (v 5.0). $P < 0.05$ was considered significant for all comparisons. Statistical significance is indicated as follows: *, $P < 0.05$; **, $P < 0.01$; ***, $P < 0.001$.

SUPPLEMENTAL MATERIAL

Supplemental material for this article may be found at http://mbio.asm.org/lookup/suppl/doi:10.1128/mBio.01476-14/-/DCSupplemental.

Figure S1, TIFF file, 0.9 MB.
Figure S2, TIFF file, 0.5 MB.
Figure S3, TIFF file, 4.3 MB.
Figure S4, TIFF file, 0.5 MB.
Figure S5, TIFF file, 0.2 MB.

ACKNOWLEDGMENTS

This work was supported by NIH grant R01 NS052632 to R.S.K. B.P.D. was supported by a National Science Foundation graduate research fellowship (DGE-1143954). L.C.O. was supported by a Ruth L. Kirschstein postdoctoral NRSA award (1F32NS0748424-01).

We thank Michael Diamond and Helen Lazear for critical insights into the manuscript and Bryan Bollman for technical assistance.

REFERENCES

1. **Persidsky Y, Ramirez SH, Haorah J, Kanmogne GD.** 2006. Blood-brain barrier: structural components and function under physiologic and pathologic conditions. J. Neuroimmune Pharmacol. 1:223–236. http://dx.doi.org/10.1007/s11481-006-9025-3.
2. **Verma S, Lo Y, Chapagain M, Lum S, Kumar M, Gurjav U, Luo H,**

Nakatsuka A, Nerurkar VR. 2009. West Nile virus infection modulates human brain microvascular endothelial cells tight junction proteins and cell adhesion molecules: transmigration across the in vitro blood-brain barrier. Virology **385:**425–433. http://dx.doi.org/10.1016/j.virol.2008.11.047.

3. **Daffis S, Samuel MA, Suthar MS, Gale M, Jr, Diamond MS.** 2008. Toll-like receptor 3 has a protective role against West Nile virus infection. J. Virol. **82:**10349–10358. http://dx.doi.org/10.1128/JVI.00935-08.
4. **Wang S, Welte T, McGargill M, Town T, Thompson J, Anderson JF, Flavell RA, Fikrig E, Hedrick SM, Wang T.** 2008. Drak2 contributes to West Nile virus entry into the brain and lethal encephalitis. J. Immunol. **181:**2084–2091. http://dx.doi.org/10.4049/jimmunol.181.3.2084.
5. **Pan W, Stone KP, Hsuchou H, Manda VK, Zhang Y, Kastin AJ.** 2011. Cytokine signaling modulates blood-brain barrier function. Curr. Pharm. Des. **17:**3729–3740. http://dx.doi.org/10.2174/138161211798220918.
6. **Wang T, Town T, Alexopoulou L, Anderson JF, Fikrig E, Flavell RA.** 2004. Toll-like receptor 3 mediates West Nile virus entry into the brain causing lethal encephalitis. Nat. Med. **10:**1366–1373. http://dx.doi.org/10.1038/nm1140.
7. **Carson PJ, Konewko P, Wold KS, Mariani P, Goli S, Bergloff P, Crosby RD.** 2006. Long-term clinical and neuropsychological outcomes of West Nile virus infection. Clin. Infect. Dis. **43:**723–730. http://dx.doi.org/10.1086/506939.
8. **Benedict CA.** 2003. Viruses and the TNF-related cytokines, an evolving battle. Cytokine Growth Factor Rev. **14:**349–357. http://dx.doi.org/10.1016/S1359-6101(03)00030-3.
9. **Stokes CA, Ismail S, Dick EP, Bennett JA, Johnston SL, Edwards MR, Sabroe I, Parker LC.** 2011. Role of interleukin-1 and MyD88-dependent signaling in rhinovirus infection. J. Virol. **85:**7912–7921. http://dx.doi.org/10.1128/JVI.02649-10.
10. **Shrestha B, Zhang B, Purtha WE, Klein RS, Diamond MS.** 2008. Tumor necrosis factor alpha protects against lethal West Nile virus infection by promoting trafficking of mononuclear leukocytes into the central nervous system. J. Virol. **82:**8956–8964. http://dx.doi.org/10.1128/JVI.01118-08.
11. **Zhang B, Patel J, Croyle M, Diamond MS, Klein RS.** 2010. TNF-alpha-dependent regulation of CXCR3 expression modulates neuronal survival during West Nile virus encephalitis. J. Neuroimmunol. **224:**28–38. http://dx.doi.org/10.1016/j.jneuroim.2010.05.003.
12. **Ramos HJ, Lanteri MC, Blahnik G, Negash A, Suthar MS, Brassil MM, Sodhi K, Treuting PM, Busch MP, Norris PJ, Gale M, Jr..** 2012. IL-1beta signaling promotes CNS-intrinsic immune control of West Nile virus infection. PLoS Pathog. **8**(**11**):e1003039. http://dx.doi.org/10.1371/journal.ppat.1003039.
13. **Durrant DM, Robinette ML, Klein RS.** 2013. IL-1R1 is required for dendritic cell-mediated T cell reactivation within the CNS during West Nile virus encephalitis. J. Exp. Med. **210:**503–516. http://dx.doi.org/10.1084/jem.20121897.
14. **Chai Q, He WQ, Zhou M, Lu H, Fu ZF.** 2014. Enhancement of blood-brain barrier permeability and reduction of tight junction protein expression are modulated by chemokines/cytokines induced by rabies virus infection. J. Virol. **88:**4698–4710. http://dx.doi.org/10.1128/JVI.03149-13.
15. **Platanias LC.** 2005. Mechanisms of type-I- and type-II-interferon-mediated signalling. Nat. Rev. Immunol. **5:**375–386. http://dx.doi.org/10.1038/nri1604.
16. **Samuel MA, Diamond MS.** 2005. Alpha/beta interferon protects against lethal West Nile virus infection by restricting cellular tropism and enhancing neuronal survival. J. Virol. **79:**13350–13361. http://dx.doi.org/10.1128/JVI.79.21.13350-13361.2005.
17. **Pinto AK, Daffis S, Brien JD, Gainey MD, Yokoyama WM, Sheehan KC, Murphy KM, Schreiber RD, Diamond MS.** 2011. A temporal role of type I interferon signaling in $CD8^+$ T cell maturation during acute West Nile virus infection. PLoS Pathog. **7**(**12**):e1002407. http://dx.doi.org/10.1371/journal.ppat.1002407.
18. **Lazear HM, Pinto AK, Vogt MR, Gale M, Jr, Diamond MS.** 2011. Beta interferon controls West Nile virus infection and pathogenesis in mice. J. Virol. **85:**7186–7194. http://dx.doi.org/10.1128/JVI.00396-11.
19. **Lazear HM, Lancaster A, Wilkins C, Suthar MS, Huang A, Vick SC, Clepper L, Thackray L, Brassil MM, Virgin HW, Nikolich-Zugich J, Moses AV, Gale M, Fruh K, Diamond MS.** 2013. IRF-3, IRF-5, and IRF-7 coordinately regulate the type I IFN response in myeloid dendritic cells downstream of MAVS signaling. PLoS Pathog. **9**(**1**):e1003118. http://dx.doi.org/10.1371/journal.ppat.1003118.
20. **Kraus J, Oschmann P.** 2006. The impact of interferon-beta treatment on the blood-brain barrier. Drug Discov. Today **11:**755–762. http://dx.doi.org/10.1016/j.drudis.2006.06.008.
21. **Markowitz CE.** 2007. Interferon-beta: mechanism of action and dosing issues. Neurology **68:**S8–11. http://dx.doi.org/10.1212/01.wnl.0000256345.01907.09.
22. **McCandless EE, Zhang B, Diamond MS, Klein RS.** 2008. CXCR4 antagonism increases T cell trafficking in the central nervous system and improves survival from West Nile virus encephalitis. Proc. Natl. Acad. Sci. U. S. A. **105:**11270–11275. http://dx.doi.org/10.1073/pnas.0800898105.
23. **Engle MJ, Diamond MS.** 2003. Antibody prophylaxis and therapy against West Nile virus infection in wild-type and immunodeficient mice. J. Virol. **77:**12941–12949. http://dx.doi.org/10.1128/JVI.77.24.12941-12949.2003.
24. **Busch MP, Kleinman SH, Tobler LH, Kamel HT, Norris PJ, Walsh I, Matud JL, Prince HE, Lanciotti RS, Wright DJ, Linnen JM, Caglioti S.** 2008. Virus and antibody dynamics in acute west Nile virus infection. J. Infect. Dis. **198:**984–993. http://dx.doi.org/10.1086/591467.
25. **Chu JJ, Ng ML.** 2003. The mechanism of cell death during West Nile virus infection is dependent on initial infectious dose. J. Gen. Virol. **84:**3305–3314. http://dx.doi.org/10.1099/vir.0.19447-0.
26. **Etienne-Manneville S, Hall A.** 2002. Rho GTPases in cell biology. Nature **420:**629–635. http://dx.doi.org/10.1038/nature01148.
27. **Szretter KJ, Daffis S, Patel J, Suthar MS, Klein RS, Gale M, Jr, Diamond MS.** 2010. The innate immune adaptor molecule MyD88 restricts West Nile virus replication and spread in neurons of the central nervous system. J. Virol. **84:**12125–12138. http://dx.doi.org/10.1128/JVI.01026-10.
28. **Pinto AK, Ramos HJ, Wu X, Aggarwal S, Shrestha B, Gorman M, Kim KY, Suthar MS, Atkinson JP, Gale M, Jr, Diamond MS.** 2014. Deficient IFN signaling by myeloid cells leads to MAVS-dependent virus-induced sepsis. PLoS Pathog. **10**(**4**):e1004086. http://dx.doi.org/10.1371/journal.ppat.1004086.
29. **Daffis S, Samuel MA, Suthar MS, Keller BC, Gale M, Diamond MS.** 2008. Interferon regulatory factor IRF-7 induces the antiviral alpha interferon response and protects against lethal West Nile virus infection. J. Virol. **82:**8465–8475. http://dx.doi.org/10.1128/JVI.00918-08.
30. **Tsao N, Hsu HP, Wu CM, Liu CC, Lei HY.** 2001. Tumour necrosis factor-alpha causes an increase in blood-brain barrier permeability during sepsis. J. Med. Microbiol. **50:**812–821.
31. **Wong D, Dorovini-Zis K, Vincent SR.** 2004. Cytokines, nitric oxide, and cGMP modulate the permeability of an in vitro model of the human blood-brain barrier. Exp. Neurol. **190:**446–455. http://dx.doi.org/10.1016/j.expneurol.2004.08.008.
32. **Phares TW, Kean RB, Mikheeva T, Hooper DC.** 2006. Regional differences in blood-brain barrier permeability changes and inflammation in the apathogenic clearance of virus from the central nervous system. J. Immunol. **176:**7666–7675. http://dx.doi.org/10.4049/jimmunol.176.12.7666.
33. **Forster C, Burek M, Romero IA, Weksler B, Couraud PO, Drenckhahn D.** 2008. Differential effects of hydrocortisone and TNFalpha on tight junction proteins in an *in vitro* model of the human blood-brain barrier. J. Physiol. **586:**1937–1949. http://dx.doi.org/10.1113/jphysiol.2007.146852.
34. **Minagar A, Long A, Ma T, Jackson TH, Kelley RE, Ostanin DV, Sasaki M, Warren AC, Jawahar A, Cappell B, Alexander JS.** 2003. Interferon (IFN)-beta 1a and IFN-beta1b block IFN-gamma-induced disintegration of endothelial junction integrity and barrier. Endothelium **10:**299–307. http://dx.doi.org/10.1080/714007544.
35. **Patkar C, Giaya K, Libraty DH.** 2013. Dengue virus type 2 modulates endothelial barrier function through CD73. Am. J. Trop. Med. Hyg. **88:**89–94. http://dx.doi.org/10.4269/ajtmh.2012.12-0474.
36. **Kraus J, Ling AK, Hamm S, Voigt K, Oschmann P, Engelhardt B.** 2004. Interferon-beta stabilizes barrier characteristics of brain endothelial cells in vitro. Ann. Neurol. **56:**192–205. http://dx.doi.org/10.1002/ana.20161.
37. **Guarda G, Braun M, Staehli F, Tardivel A, Mattmann C, Forster I, Farlik M, Decker T, Du Pasquier RA, Romero P, Tschopp J.** 2011. Type I interferon inhibits interleukin-1 production and inflammasome activation. Immunity **34:**213–223. http://dx.doi.org/10.1016/j.immuni.2011.02.006.
38. **Huang Y, Blatt LM, Taylor MW.** 1995. Type 1 interferon as an antiinflammatory agent: inhibition of lipopolysaccharide-induced interleukin-1beta and induction of interleukin-1 receptor antagonist. J. Interferon Cytokine Res. **15:**317–321. http://dx.doi.org/10.1089/jir.1995.15.317.
39. **Argaw AT, Zhang Y, Snyder BJ, Zhao ML, Kopp N, Lee SC, Raine CS, Brosnan CF, John GR.** 2006. IL-1beta regulates blood-brain barrier per-

meability via reactivation of the hypoxia-angiogenesis program. J. Immunol. **177:**5574–5584. http://dx.doi.org/10.4049/jimmunol.177.8.5574.
40. **Blamire AM, Anthony DC, Rajagopalan B, Sibson NR, Perry VH, Styles P.** 2000. Interleukin-1beta-induced changes in blood-brain barrier permeability, apparent diffusion coefficient, and cerebral blood volume in the rat brain: a magnetic resonance study. J. Neurosci. **20:**8153–8159.
41. **Roe K, Kumar M, Lum S, Orillo B, Nerurkar VR, Verma S.** 2012. West Nile virus-induced disruption of the blood-brain barrier in mice is characterized by the degradation of the junctional complex proteins and increase in multiple matrix metalloproteinases. J. Gen. Virol. **93:**1193–1203. http://dx.doi.org/10.1099/vir.0.040899-0.
42. **Morrey JD, Olsen AL, Siddharthan V, Motter NE, Wang H, Taro BS, Chen D, Ruffner D, Hall JO.** 2008. Increased blood-brain barrier permeability is not a primary determinant for lethality of West Nile virus infection in rodents. J. Gen. Virol. **89:**467–473. http://dx.doi.org/10.1099/vir.0.83345-0.
43. **Dai J, Wang P, Bai F, Town T, Fikrig E.** 2008. Icam-1 participates in the entry of west Nile virus into the central nervous system. J. Virol. **82:**4164–4168. http://dx.doi.org/10.1128/JVI.02621-07.
44. **Arjona A, Foellmer HG, Town T, Leng L, McDonald C, Wang T, Wong SJ, Montgomery RR, Fikrig E, Bucala R.** 2007. Abrogation of macrophage migration inhibitory factor decreases West Nile virus lethality by limiting viral neuroinvasion. J. Clin. Invest. **117:**3059–3066. http://dx.doi.org/10.1172/JCI32218.
45. **Schafer A, Brooke CB, Whitmore AC, Johnston RE.** 2011. The role of the blood-brain barrier during Venezuelan equine encephalitis virus infection. J. Virol. **85:**10682–10690. http://dx.doi.org/10.1128/JVI.05032-11.
46. **Glass WG, Lim JK, Cholera R, Pletnev AG, Gao JL, Murphy PM.** 2005. Chemokine receptor CCR5 promotes leukocyte trafficking to the brain and survival in West Nile virus infection. J. Exp. Med. **202:**1087–1098. http://dx.doi.org/10.1084/jem.20042530.
47. **Klein RS, Lin E, Zhang B, Luster AD, Tollett J, Samuel MA, Engle M, Diamond MS.** 2005. Neuronal CXCL10 directs $CD8^+$ T-cell recruitment and control of West Nile virus encephalitis. J. Virol. **79:**11457–11466. http://dx.doi.org/10.1128/JVI.79.17.11457-11466.2005.
48. **Shrestha B, Diamond MS.** 2004. Role of $CD8^+$ T cells in control of West Nile virus infection. J. Virol. **78:**8312–8321. http://dx.doi.org/10.1128/JVI.78.15.8312-8321.2004.
49. **Lim JK, Obara CJ, Rivollier A, Pletnev AG, Kelsall BL, Murphy PM.** 2011. Chemokine receptor Ccr2 is critical for monocyte accumulation and survival in West Nile virus encephalitis. J. Immunol. **186:**471–478. http://dx.doi.org/10.4049/jimmunol.1003003.
50. **Town T, Bai F, Wang T, Kaplan AT, Qian F, Montgomery RR, Anderson JF, Flavell RA, Fikrig E.** 2009. Toll-like receptor 7 mitigates lethal West Nile encephalitis via interleukin 23-dependent immune cell infiltration and homing. Immunity **30:**242–253. http://dx.doi.org/10.1016/j.immuni.2008.11.012.
51. **Lazear HM, Pinto AK, Ramos HJ, Vick SC, Shrestha B, Suthar MS, Gale M, Jr, Diamond MS.** 2013. Pattern recognition receptor MDA5 modulates $CD8^+$ T cell-dependent clearance of West Nile virus from the central nervous system. J. Virol. **87:**11401–11415. http://dx.doi.org/10.1128/JVI.01403-13.
52. **Diamond MS, Gale M, Jr..** 2012. Cell-intrinsic innate immune control of West Nile virus infection. Trends Immunol. **33:**522–530. http://dx.doi.org/10.1016/j.it.2012.05.008.
53. **Xia J, Winkelmann ER, Gorder SR, Mason PW, Milligan GN.** 2013. TLR3- and MyD88-dependent signaling differentially influences the development of West Nile virus-specific B cell responses in mice following immunization with RepliVAX WN, a single-cycle flavivirus vaccine candidate. J. Virol. **87:**12090–12101. http://dx.doi.org/10.1128/JVI.01469-13.
54. **Wang P, Dai J, Bai F, Kong KF, Wong SJ, Montgomery RR, Madri JA, Fikrig E.** 2008. Matrix metalloproteinase 9 facilitates West Nile virus entry into the brain. J. Virol. **82:**8978–8985. http://dx.doi.org/10.1128/JVI.00314-08.
55. **Verma S, Kumar M, Gurjav U, Lum S, Nerurkar VR.** 2010. Reversal of West Nile virus-induced blood-brain barrier disruption and tight junction proteins degradation by matrix metalloproteinases inhibitor. Virology **397:**130–138. http://dx.doi.org/10.1016/j.virol.2009.10.036.
56. **Persidsky Y, Heilman D, Haorah J, Zelivyanskaya M, Persidsky R, Weber GA, Shimokawa H, Kaibuchi K, Ikezu T.** 2006. Rho-mediated regulation of tight junctions during monocyte migration across the blood-brain barrier in HIV-1 encephalitis (HIVE). Blood **107:**4770–4780. http://dx.doi.org/10.1182/blood-2005-11-4721.
57. **Gea-Banacloche J, Johnson RT, Bagic A, Butman JA, Murray PR, Agrawal AG.** 2004. West Nile virus: pathogenesis and therapeutic options. Ann. Intern. Med. **140:**545–553. http://dx.doi.org/10.7326/0003-4819-140-7-200404060-00015.
58. **Kalil AC, Devetten MP, Singh S, Lesiak B, Poage DP, Bargenquast K, Fayad P, Freifeld AG.** 2005. Use of interferon-alpha in patients with West Nile encephalitis: report of 2 cases. Clin. Infect. Dis. **40:**764–766. http://dx.doi.org/10.1086/427945.
59. **Winston DJ, Vikram HR, Rabe IB, Dhillon G, Mulligan D, Hong JC, Busuttil RW, Nowicki MJ, Mone T, Civen R, Tecle SA, Trivedi KK, Hocevar SN, Nile W, Virus Transplant-Associated Transmission Investigation Team.** 2014. Donor-derived West Nile virus infection in solid organ transplant recipients: report of four additional cases and review of clinical, diagnostic, and therapeutic features. Transplantation **97:**881–889. http://dx.doi.org/10.1097/TP.0000000000000024.
60. **Bigham AW, Buckingham KJ, Husain S, Emond MJ, Bofferding KM, Gildersleeve H, Rutherford A, Astakhova NM, Perelygin AA, Busch MP, Murray KO, Sejvar JJ, Green S, Kriesel J, Brinton MA, Bamshad M.** 2011. Host genetic risk factors for West Nile virus infection and disease progression. PLoS One **6**(9):e24745. http://dx.doi.org/10.1371/journal.pone.0024745.
61. **Lim JK, Lisco A, McDermott DH, Huynh L, Ward JM, Johnson B, Johnson H, Pape J, Foster GA, Krysztof D, Follmann D, Stramer SL, Margolis LB, Murphy PM.** 2009. Genetic variation in OAS1 is a risk factor for initial infection with West Nile virus in man. PLoS Pathog. **5**(2):e1000321. http://dx.doi.org/10.1371/journal.ppat.1000321.
62. **Kong KF, Delroux K, Wang X, Qian F, Arjona A, Malawista SE, Fikrig E, Montgomery RR.** 2008. Dysregulation of TLR3 impairs the innate immune response to West Nile virus in the elderly. J. Virol. **82:**7613–7623. http://dx.doi.org/10.1128/JVI.00618-08.
63. **Ebel GD, Dupuis AP, 2nd, Ngo K, Nicholas D, Kauffman E, Jones SA, Young D, Maffei J, Shi PY, Bernard K, Kramer LD.** 2001. Partial genetic characterization of West Nile virus strains, New York State, 2000. Emerg. Infect. Dis. **7:**650–653. http://dx.doi.org/10.3201/eid0704.017408.
64. **Diamond MS, Shrestha B, Marri A, Mahan D, Engle M.** 2003. B cells and antibody play critical roles in the immediate defense of disseminated infection by West Nile encephalitis virus. J. Virol. **77:**2578–2586. http://dx.doi.org/10.1128/JVI.77.4.2578-2586.2003.
65. **Szretter KJ, Daniels BP, Cho H, Gainey MD, Yokoyama WM, Gale M, Jr, Virgin HW, Klein RS, Sen GC, Diamond MS.** 2012. 2′-O methylation of the viral mRNA cap by West Nile virus evades ifit1-dependent and -independent mechanisms of host restriction *in vivo*. PLoS Pathog. **8**(5):e1002698. http://dx.doi.org/10.1371/journal.ppat.1002698.
66. **Patel JR, McCandless EE, Dorsey D, Klein RS.** 2010. CXCR4 promotes differentiation of oligodendrocyte progenitors and remyelination. Proc. Natl. Acad. Sci. U. S. A. **107:**11062–11067. http://dx.doi.org/10.1073/pnas.1006301107.
67. **Daniels BP, Cruz-Orengo L, Pasieka TJ, Couraud PO, Romero IA, Weksler B, Cooper JA, Doering TL, Klein RS.** 2013. Immortalized human cerebral microvascular endothelial cells maintain the properties of primary cells in an in vitro model of immune migration across the blood brain barrier. J. Neurosci. Methods **212:**173–179. http://dx.doi.org/10.1016/j.jneumeth.2012.10.001.
68. **Cruz-Orengo L, Daniels BP, Dorsey D, Basak SA, Grajales-Reyes JG, McCandless EE, Piccio L, Schmidt RE, Cross AH, Crosby SD, Klein RS.** 2014. Enhanced sphingosine-1-phosphate receptor 2 expression underlies female CNS autoimmunity susceptibility. J. Clin. Invest. **124:**2571–2584. http://dx.doi.org/10.1172/JCI73408.